Geosci. Model Dev. Discuss., 8, 4051–4073, 2015
www.geosci-model-dev-discuss.net/8/4051/2015/
doi:10.5194/gmdd-8-4051-2015

Geoscientific Model Development Discussions
Open Access

Photolysis rates in correlated overlapping cloud fields: Cloud-J 7.3

M. J. Prather

Earth System Science Department, UC Irvine California, USA

Received: 29 April 2015 – Accepted: 6 May 2015 – Published: 27 May 2015

Correspondence to: M. J. Prather (mprather@uci.edu)

Published by Copernicus Publications on behalf of the European Geosciences Union.

Abstract

A new approach for modeling photolysis rates (J values) in atmospheres with fractional cloud cover has been developed and implemented as Cloud-J – a multi-scattering eight-stream radiative transfer model for solar radiation based on Fast-J. Using observed statistics for the vertical correlation of cloud layers, Cloud-J 7.3 provides a practical and accurate method for modeling atmospheric chemistry. The combination of the new maximum-correlated cloud groups with the integration over all cloud combinations represented by four quadrature atmospheres produces mean J values in an atmospheric column with root-mean-square errors of 4 % or less compared with 10–20 % errors using simpler approximations. Cloud-J is practical for chemistry-climate models, requiring only an average of 2.8 Fast-J calls per atmosphere, vs. hundreds of calls with the correlated cloud groups, or 1 call with the simplest cloud approximations. Another improvement in modeling J values, the treatment of volatile organic compounds with pressure-dependent cross sections is also incorporated into Cloud-J.

1 Introduction

Photolysis, the dissociation of molecules upon absorbing sunlight, drives atmospheric chemistry and controls the composition of the air we breathe. Photolysis rates are governed by the intensity of sunlight, which is altered by scattering and absorption processes within the atmosphere. Clouds, aerosols, and gases control these processes; but ambiguity in the representation of clouds in atmospheric models is currently the largest source of uncertainty in photolysis rates. This paper presents a new, pragmatic approach for representing the overlap of clouds derived from observations and cloud models, and then provides several practical approximations with marginal computational costs that can be readily incorporated in atmospheric chemistry models. This computer code is a major expansion of Fast-J (Wild et al., 2000; Bian and Prather, 2002; Neu et al., 2007) and is presented here as Cloud-J 7.3 (Cloud-J contains Fast-J

GMDD
8, 4051–4073, 2015

and thus continues that numbering sequence, for which Fast-J 7.2 was the last released version.)

Clouds can increase photolysis rates through scattered sunlight, but they can greatly reduce them by shadowing. Modeling the scattering by cloud layers in a column atmosphere and resulting photolysis rates is practical, as in Fast-J, if the layers are horizontally uniform across the modeled air parcel (defined typically as a rectilinear box bounded by latitude, longitude and pressure surfaces). Clouds layers, however, have horizontal scales of a few kilometers (Slobodda et al., 2015), and thus are represented in global and regional models as fractional coverage in each parcel. In calculating the average photolysis or heating rates through the column atmosphere, one must know how the cloud fractions overlap. Early modeling assumed that model layers consisted of maximally overlapped groups (MAX) that would be randomly overlapped relative to one another (MAX-RAN) (Briegleb, 1992; Feng et al., 2004). A more accurate description of cloud overlap is that clouds are correlated throughout the column atmosphere with a correlation length ranging from 1.5 to 3 km in height (Pincus et al., 2005; Naud and DelGenio, 2006; Kato et al., 2010; Oreopoulis et al., 2012).

A practical application of this cloud overlap information, merging maximally overlapped groups that are correlated with each other (MAX-COR) is defined in Sect. 2, where the impact of cloud overlap models on photolysis rates (J values) is also shown. Cloud overlap models generate statistics that lead to a large number of weighted independent column atmospheres (ICAs), where the number is too large to be used directly to calculate photolysis or heating rates in global models. Section 3 looks at the simple cloud models and the approaches to approximate the sum over ICAs, examining their errors. Another recent development in modeling photolysis rates included with Cloud-J is the treatment of volatile organic compounds with pressure-dependent cross sections, presented in Sect. 4. Recommendations for the cloud-overlap model and the ICA-approximation method are discussed in Sect. 5.

GMDD
8, 4051–4073, 2015

2 Overlap models for fractionally cloudy atmospheres

Typically, meteorological forecasts or climate models used in atmospheric chemistry models report fractionally cloudy atmospheres (FCAs) in each grid-square. Computation of the photolysis or heating rates in an FCA requires knowledge of how the clouds in each layer overlap. The calculation of J values in most atmospheric chemistry models today involves solving the radiative transfer equations in a plane-parallel atmosphere where the vertical layers can be highly inhomogeneous but the horizontal planes are uniform (Stamnes et al., 1988; Wild et al., 2000; Tie et al., 2003). Thus, the only workable method (other than 3-D radiative transfer) is to represent the FCA by a number of independent column atmospheres (ICAs) where each ICA is either 100 % cloudy or clear in each layer. The fractional cloud overlap model determines the layer-structure, weighting, and number of ICAs. Other simple cloud models approximated overlap by: (i) ignoring clouds entirely (clear sky), (ii) averaging the fractional cloud, f, over each layer, conserving total cloud water (average clouds); and (iii) increasing the cloud fraction by using $f^{3/2}$, increasing the total cloud water in proportion, and then averaging over the layer (Briegleb, 1992). These methods will be compared with cloud overlap models in Sect. 3. Here, we focus on how the ICAs differ across cloud overlap models.

2.1 Random overlap (RAN)

The ways in which fractionally cloudy layers can overlap is shown schematically in Fig. 1. One assumption is random overlap (RAN). In this case the likelihood (fractional weight, w) of having the cloud in layer L1 fall below the cloud in layer L2 is random and hence equals f^{L1}. This particular pairing – cloud below cloud – becomes ICA #1. Superscripts in the equations below refer to atmospheric layers. The likelihood for the

GMDD
8, 4051–4073, 2015

clear layer under the cloudy layer is by default the complement.

$$w^{L1}(\#1) = f^{L1} \quad (1)$$

$$w^{L1}(\#2) = 1 - f^{L1} \quad (2)$$

The likelihood of the cloudy layer in L2 above is

$$w^{L2}(\#1) = w^{L2}(\#2) = f^{L2} \quad (3)$$

The total weight W for each ICA #1 and #2 is then the product of w^{L1} and w^{L2}.

$$W^{L1-L2}(\#1) = w^{L1}(\#1)w^{L2}(\#1) = f^{L1}f^{L2} = 0.15 \times 0.20 = 3\,\% \text{ (from Fig. 1)} \quad (4)$$

$$W^{L1-L2}(\#2) = w^{L1}(\#2)w^{L2}(\#2) = (1 - f^{L1})f^{L2} = 0.85 \times 0.20 = 17\,\% \quad (5)$$

Similar rules apply to ICAs #3 and #4,

$$w^{L1}(\#3) = f^{L1} \quad \text{and} \quad w^{L2}(\#3) = 1 - f^{L2} \quad (6)$$

$$w^{L1}(\#4) = 1 - f^{L1} \quad \text{and} \quad w^{L2}(\#4) = 1 - f^{L2}. \quad (7)$$

and thus

$$W^{L1-L2}(\#3) = w^{L1}(\#3)w^{L2}(\#3) = f^{L1}(1 - f^{L2}) = 0.15 \times 0.80 = 12\,\% \text{ (Fig. 1)} \quad (8)$$

$$W^{L1-L2}(\#4) = w^{L1}(\#4)w^{L2}(\#4) = (1 - f^{L1})(1 - f^{L2}) = 0.85 \times 0.80 = 68\,\% \quad (9)$$

ICAs #1 and #3 are tagged as cloudy in L1, and ICAs #2 and #4 are tagged as clear in L1. The sum of cloudy fractions in L1 must be conserved: 3 % + 12 % = 15 % = f^{L1}. One of the problems in implementing a full RAN model is that the number of ICAs scales as 2^{NL}, where NL is the number of cloudy layers in the RAN group.

GMDD
8, 4051–4073, 2015

2.2 Correlated overlap (COR)

When correlated, the likelihood of a cloudy layer underlying another cloud is greater than random, $w^{L1}(\#1) > f^{L1}$, by a factor $g > 1$. The correlation coefficient cc ranges from 0 (random) to 1 (maximal overlap).

$$g = 1 + \mathrm{cc}(1/f^{L2} - 1), \text{ subject to } g \le 1/f^{L1} \text{ and } g \le 1/f^{L2} \tag{10}$$

Hence for cc > 0 we have increased likelihood of the cloud in L1 falling underneath the cloud in L2. For the example in Fig. 1, cc = 1/2 and $g = 3$.

$$w^{L1}(\#1) = gf^{L1} = 3 \times 0.15 = 45\,\% \tag{11}$$

$$w^{L1}(\#2) = 1 - gf^{L1} = 1 - 0.45 = 55\,\% \tag{12}$$

The likelihood of clouds in L1 falling below the clear section in L2 are reduced and calculated from the requirement that the sum of cloudy fractions in L1 is still f^{L1}.

$$w^{L1}(\#3) = f^{L1}(1 - gf^{L2})/(1 - f^{L2}) = 0.15 \times (1 - 3 \times 0.20)/0.80 = 7.5\,\% \tag{13}$$

By complement, the weighting of clear sky in layer L1 under clear sky in layer L2 is

$$w^{L1}(\#4) = 1 - w^{L1}(\#3) = 1 - 0.075 = 92.5\,\% \tag{14}$$

Note that if $cc = 0$, or $f^{L2} = 1$, or $f^{L1} = 1$, then $g = 1$ and COR defaults to RAN. The two additional limits on g in Eq. (10) are required to keep $w^{L1}(\#2)$ and $w^{L1}(\#3)$ positive. The w^{L2} weights remain simply

$$w^{L2}(\#1) = w^{L2}(\#2) = f^{L2} \tag{15}$$

$$w^{L2}(\#3) = w^{L2}(\#4) = (1 - f^{L2}). \tag{16}$$

GMDD
8, 4051–4073, 2015

The combined ICA weights are

$$W^{L1-L2}(\#1) = w^{L1}(\#1)w^{L2}(\#1) = gf^{L1}f^{L2} = 3 \times 0.15 \times 0.20 = 9\,\% \quad (17)$$

$$W^{L1-L2}(\#2) = w^{L1}(\#2)w^{L2}(\#2) = (1 - gf^{L1})f^{L2} = 0.55 \times 0.20 = 11\,\% \quad (18)$$

$$W^{L1-L2}(\#3) = w^{L1}(\#3)w^{L2}(\#3) = f^{L1}(1 - gf^{L2}) = 0.15 \times 0.40 = 6\,\% \quad (19)$$

$$W^{L1-L2}(\#4) = w^{L1}(\#4)w^{L2}(\#4) = 1 - f^{L2} - f^{L1}(1 - gf^{L2}) = 1 - 0.20 - 0.06 = 74\,\% \quad (20)$$

As in RAN, ICAs #1 and #3 are tagged as cloudy in layer L1, and ICAs #2 and #4 are tagged as clear in layer L1, and the sum of cloudy fractions is conserved ($9\,\% + 6\,\% + 15\,\% = f^{L1}$), but with different weightings. The COR model also has ICAs scaling as 2^{NL}.

2.3 Maximal overlap (MAX)

For maximal overlap of clouds (MAX) as in Fig. 1, the two layers L1 and L2 form a MAX group G1 consisting of 1 clear-sky column (80 % fractional coverage) and 2 cloudy columns – one with clouds in both layers (15 %) and one with a cloud only in the upper layer L2 (5 %). The clear-sky column does not occur if any of the MAX layers has a cloud fraction of 100 %. For continuous cloud fractions, the number of ICAs equals the number of different cloud fractions present (plus 1 if clear sky present), and thus it scales as NL, the number of layers in the MAX group. A MAX group is characterized by the number of unique cloudy fractions (f_1, f_2, f_3, ...) and their weights (w_1, w_2, w_3, ...) with a cloudy sum $F = \sum f_i \leq 1$ and a (possible) clear-sky column of fraction $1 - F$. As in the earlier Fast-J work (Neu et al., 2007), the cloud fractions in Cloud-J are quantized to limit the number of ICAs in a MAX group. The examples here use 10 bins, and hence cloud fractions are limited to 0, 10, 20, 30,..., 100 %. With this binning, the in-cloud water content is scaled to conserve the cloud water content in each layer. This approximation is then resolution independent in terms of the number of model layers and limits each MAX group to 10 ICAs.

GMDD
8, 4051–4073, 2015

2.4 Maximal groups with correlated overlap (MAX-COR)

The MAX-COR model generates ICAs from upper and lower layers that are MAX groups. For a general approach, we will assume that the upper group G2 consists of N2 cloudy columns (members) with fractions $f^{G2}_{J2=1:N2}$ totaling F^{G2} and 1 clear-sky column (member) of fraction $1 - F^{G2}$. Likewise, the lower group G1 has N1 cloudy members with fractions $f^{G1}_{J1=1:N1}$ totaling F^{G1} and a clear-sky with fraction $1 - F^{G1}$. Each of the cloudy members in group G1, $f^{G1}_{J1=1:N1}$, will be paired with N2 (cloudy) + 1 (clear) member above. The number of ICAs will be (N1 + 1) (N2 + 1), assuming that there are clear-sky members in both groups. The ICA sequence (J1, J2) is then

$$(1,1),(2,1),(3,1),\ldots(N1+1,1),(1,2),(2,2),(3,2),\ldots(N1+1,N2+1) \quad (21)$$

such that ICA #M is composed of members

$$J1 = (M-1) \bmod (N1+1) + 1 \quad (22)$$

$$J2 = \text{integer}\,((M-1)/(N1+1)) \bmod (N2+1) + 1 \quad (23)$$

The correlation factor is same for all members, derived from the total cloudy fractions F^{G1} and F^{G2}.

$$g = 1 + \text{cc}\,(1/F^{G2} - 1), \text{ subject to } g \le 1/F^{G1} \text{ and } g \le 1/F^{G2} \quad (24)$$

For convenience denote $J1 \le N1$ as cloudy^{G1}, $J1 = N1 + 1$ as clear^{G1}, $J2 \le N2$ as cloudy^{G2}, and $J2 = N2 + 1$ as clear^{G2}. Then the weightings for the G1 members are

$$w^{G1}(\text{cloudy}^{G1}, \text{cloudy}^{G2}) = g f^{G1}_{J1} \quad (25)$$

$$w^{G1}(\text{clear}^{G1}, \text{cloudy}^{G2}) = 1 - \sum_{J1=1:N1} g f^{G1}_{J1} = 1 - g F^{G1} \quad (26)$$

GMDD
8, 4051–4073, 2015

Conserving each cloudy group member's fractional area in G1 gives the weights under G2 clear sky.

$$w^{G1}(\text{cloudy}^{G1}, \text{clear}^{G2}) = f_{J1}^{G1}(1 - gF^{G2})/(1 - F^{G2}) \quad (27)$$

$$w^{G1}(\text{clear}^{G1}, \text{clear}^{G2}) = 1 - F^{G1}(1 - gF^{G2})/(1 - F^{G2}) \quad (28)$$

All of these formulae work also if $F^{G1} > F^{G2}$, and if $F^{G1} = 0$ or 1 (same for F^{G2}). A special case of MAX-COR is MAX-RAN when cc = 0. With the cloud fractions binned into 10 intervals, then the number of ICAs for MAX-COR or MAX-RAN models scales as 10^{NG}, where NG is the number of MAX groups.

2.5 *J* value errors

Our recommended cloud overlap model uses the information on vertical correlations (Pincus et al., 2005; Naud and DelGenio, 2006; Kato et al., 2010; Oreopoulis et al., 2012), which shows correlations lengths of order 1.5 km in the lowest layers increasing to 3 km or more in the upper troposphere. Since a true COR model will scale as 2^{NL} and becomes rapidly impractical for high-resolution models, we define 6 MAX groups as those layers within a correlation length: 0–1.5 km altitude, 1.5–3.5, 3.5–6, 6–9, 9–13, and > 13 km. The MAX groups collapse if there are no cloud fractions within the layers of the group. In looking at how this model aligned the clouds for realistic FCAs, we found that extensive cirrus fractions in the uppermost layers prevented the correlation of small-fraction cumulus below. Thus a 7th MAX group was added if there was a cirrus shield (defined from top down as adjacent ice-only clouds with $f > 0.5$). We chose a correlation factor cc = 0.33, similar to one e-fold, between groups, as the groups are chosen to be separated by about one correlation length. This model is denoted G6/.33. Two other G6 models were tested: cc = 0.00 corresponds to MAX-RAN (G6/.00); and cc = 0.99 is close to one large MAX group (G6/.99). Because of the cloud-fraction bins and the fixed correlation-length groups, the number of ICAs is bounded by 5×10^6 (including the cirrus shield). This limit is resolution independent and was never reached

GMDD
8, 4051–4073, 2015

in any FCAs examined here (highest number of ICAs for one FCA was 3500). The major computational cost comes with the Fast-J computation, and the methods for approximating the average of J values over all ICAs (Sect. 3) requires at most 4 Fast-J calculations no matter how many ICAs.

Two other cloud overlap models tested here are the MAX-RAN groupings, the same or similar to earlier work (Feng et al., 2004; Neu et al., 2007). The model G0 declares all adjacent cloudy layers to be a MAX group, and all such groups separated by a clear layer to be RAN overlapped. This model has the potential to be unstable with increasing layers as alternating clear and cloud layers results in $2^{NL/2}$ ICAs. In our tests using meteorological data with NL = 36, the maximum number of ICAs, 375, was well below this limit. The model G3 declares MAX groups by 3 atmospheric regimes: 0–1.5 km altitude as stratus-like clouds, 1.5 km to the uppermost mixed-phase clouds as cumulus-like clouds, and all ice-only cirrus-like clouds. With cloud-fraction bins, this model is limited to 10^3 ICAs, independent of vertical resolution, and had a maximum of 288 ICAs in our tests.

Our best cloud overlap model is G6/.33 since it is based on the observed-modeled cloud correlations. For a given FCA, we treat the J values calculated by summing Fast-J over all the ICAs generated by G6/.33 as the correct value. We calculate errors for the other cloud-overlap models (here) or various ICA-approximation models using the G6/.33 model (Sect. 3). The errors in photolysis rates are calculated for different cloud overlap models by generating all the ICAs, using Fast-J to calculate J values, and computing the weighted sum of J's. This study focuses on two J values that are critical in tropospheric chemistry and emphasize different wavelength ranges from near 300 nm, where O_3 absorption and molecular scattering are important, to 600 nm, where clouds are the predominant factor. J-O^1D refers to the photolysis rate of $O_3 + h\nu \Rightarrow O_2 + O(^1D)$; and J-$NO_3$ includes both channels of the rate $NO_3 + h\nu \Rightarrow NO + O_2$ and $NO_2 + O$. We tested other key J values like those of HNO_3 and NO_2, but found that their errors fell between the first two.

GMDD
8, 4051–4073, 2015

The J value tests are summarized in Table 1. We use a high-resolution snapshot from the European Center for Medium-range Weather Forecasts, similar to what is used (at lower resolution) in the UC Irvine and University of Oslo chemistry-transport models (Sovde et al., 2012; Hsu and Prather, 2014). The 640 FCAs are a 3 h average of a single longitudinal belt just above the equator (T319L60 Cycle 36) and have clouds only in the lowermost 36 layers. Profiles of temperature and ozone are taken from tropical mean observations; the Rayleigh-scattering optical depth at 600 nm is about 0.12; and a mix of aerosol layers has total optical depth of 0.23. J value errors are calculated separately for each FCA and then averaged. The number of ICAs per FCA averages 169 for model G6, 21 for model G3 and 19 for model G0; see Fig. 2 for the probability distribution of ICA numbers. Errors are pressure-weighted and include the average error over 0–1 km altitude, the root-mean-square (rms) error over 0–1 km, and the full tropospheric rms error (0–16 km). The average 0–1 km differences across the models is small (< 2 %), but the rms 0–1 and 0–16 differences are large, indicating that 640 different FCAs produce canceling errors in the mean. The rms errors for G0 and G3 are worrisome, more than 15 % in the boundary layer and 5 to 11 % in the full troposphere. The G6 errors are almost linear with the *cc* value. The G6/.99 with highly correlated overlap is similar to G3 which has MAX overlap throughout most of the atmosphere. The G6/.00 with random overlap is the closest to the correlated model G6/0.33.

3 Approximating the exact sum over ICAs

Quadrature column atmospheres (QCAs) have been defined previously (Neu et al., 2007) as 4 representative ICA-like atmospheres that represent 4 domains of ICAs with total cloud optical depths at 600 nm of 0 to 0.5 (clear sky), 0.5 to 4 (cirrus-like), 4 to 30 (stratus-like), and > 30 (cumulus-like). The original model sorted the ICA optical depths to get the weightings of each QCA and then picked the ICA that occurred at the mid-point in terms of fractional area (MdQCA). Thus there could 4 separate calls to Fast-J

GMDD
8, 4051–4073, 2015

for each of the QCAs, but on average there are 2.8 QCAs per FCA. Here we extend that work with three new methods for approximating the integral over ICAs: define each QCA from the average ICAs in its domain (AvQCA); use the averaged direct solar beam from all ICAs to derive an effective scattering optical depth from clouds in each layer (AvDir); and, a model with comparable computation cost to the QCAs, select 3 random ICAs based on their weights (Ran-3).

The AvQCA model comes easily from the MdQCA formalism, but all ICAs in each of the 4 total optical depth domains are used to calculate the average cloud-water content in each QCA. The AvDir model calculates the weighted direct solar beam from each ICA, where only 600 nm cloud extinction is included. In this case it was found that an equivalent isotropic extinction is needed as in two-stream methods (Joseph et al., 1976), and we scaled the optical depth of each cloud layer by a factor: $1–1.1 \times P_1/3$, with a minimum value of 0.04. P_1 (3 times the asymmetry factor) is the second term in the Legendre expansion of the scattering phase function for the cloud in that layer. The derived optical depth in each layer is calculated from the reduction in direct beam across the layer (Beer–Lambert Law) and put into the single Fast-J calculation with the original cloud properties of that layer, not the equivalent isotropic properties.

In addition to these ICA approximations, we also compare the G6/.33 exact sum over ICAs with three simple cloud models often use in chemistry models that do not generate ICAs: clear sky (ClSky); averaged cloud over each layer (AvCld); and cloud fraction to the 3/2 ($f^{3/2}$, CF3/2).

A sample of mean and rms errors for the seven approximate methods is given in Table 1. In addition, a tropospheric profile of the mean bias in J values is shown is Fig. 3. As expected the ClSky and AvCld methods show opposite biases and large RMS errors. The CF3/2 method produces reasonable averages, but still has rms errors of 10 % or more. The AvDir method did not perform as well as expected and looks only slightly better than CF3/2; however, the profile of mean error (Fig. 3) is preferable to that of CF3/2. Both QCA methods performed excellently and deliver rms errors less than 5 % with mean biases in the boundary layer of order ±1 %. The new AvQCA method

GMDD
8, 4051–4073, 2015

has smaller rms errors for the cases in Table 1, but the original MdQCA method may have a better profile for the mean error. Ran-3 is computationally comparable to the QCAs and has a reasonable mean bias, but the rms error is much worse, typically 10 % more.

4 Cloud-J and volatile organic compounds

Volatile organic compounds (VOCs) cover a wide class of gaseous species containing C, H, O and sometimes N or S. They play a major role in the chemical reactivity of the troposphere, including production and loss of O_3 and loss of CH_4 (e.g., Jacob et al., 1993; Horowitz et al., 1998; Ito et al., 2009; Emmons et al., 2010), plus the formation of secondary organic aerosols (SOA, e.g., Ito et al., 2007; Fu et al., 2008; Galloway et al., 2011). For most VOCs (and H_2O_2) photolysis is the dominant loss, see Fig. 4. Daily photolysis rates (loss frequencies) range from 0.03 to 20 per day and some vary greatly with altitude. For 9 of the 14 species shown in Fig. 4, the photolysis rates are larger or comparable to the loss rates for reaction with OH (given in the legend). Thus, accurate calculation of their J values is important in atmospheric chemistry models.

VOCs present a particular problem for any photolysis code that averages over wavelength intervals. For most chemical species, cross sections including quantum yields are parameterized as a function of wavelength (v) and temperature (T) (e.g., Atkinson et al., 2008; Sander et al., 2011). In this case, Fast-J calculates solar-flux-weighted, average cross sections for each wavelength bin (Wild et al., 2000; Bian and Prather, 2002). These tables are created for a set of fixed Ts, and then the cross section used for each bin in each atmospheric layer is interpolated in T. Many VOCs have complex, pressure-dependent quantum yields (e.g., Blitz et al., 2006) that follow the Stern–Volmer formulation where photolysis cross sections (for dissociation) are a function of wavelength, temperature, and pressure (P), typically of the form $A(T,v)/(1+B(T,v)P)$, where A and B can be rational polynomial functions of T and v (see Sander et al., 2011). For most VOCs the pressure dependence changes across the wavelengths

GMDD
8, 4051–4073, 2015

within a model bin and thus the T dependence averaged cross sections will have different values at different P, but cannot be simply post-interpolated as a function of P because of the wavelength dependence of B. A two-dimensional set of cross sections for each wavelength bin, interpolated as a function of T and P, could be developed but would add to the complexity and cost of Fast-J.

Recognizing that VOCs are predominantly tropospheric and that T and P are highly correlated in the troposphere, Cloud-J, and the new Fast-J that sits within it, have devised an alternative method of interpolating the cross sections for each atmospheric layer: T is the traditional method used for most species; but P is used for VOCs with highly pressure-dependent quantum yields. For P interpolation, the cross sections are averaged over wavelength at 3 points along a typical tropospheric lapse rate: (0 km, 295 K, 999 hPa); (5 km, 272 K, 566 hPa); and (13 km, 220 K, 177 hPa). Currently species with P interpolation include: acetaldhyde, methylvinyl ketone, methylethyl ketone, glyoxal, methyl glyoxal, and one branch of acetone photolysis. Fast-J does not extrapolate beyond its supplied tables, and thus currently it applies 177 hPa cross sections for these VOCs throughout the stratosphere, but this should have minimal impact on stratospheric chemistry. Depending on the available laboratory data, the number of cross-section tables per species in the new Fast-J (either T or P interpolation) can be 1, 2, or 3. Cloud-J, new with version 7.3, includes an updated version of Fast-J version 7.1, whose only change is in the formatting of the input files to allow for more flexible numbering and labeling of species with their cross sections and of the cloud-aerosol scattering tables.

5 Discussion and recommendations

We recommend use of the G6/.33 MAX-COR model for cloud overlap with AvQCA to approximate the average photolysis rates over the ICAs. This combination of algorithms best matches the exact solution for average J values. Averaging J values for an air parcel that includes a mix of cloudy and clear air is not the same as averaging the

GMDD
8, 4051–4073, 2015

chemical reactivity across cloudy and clear. Nevertheless, for species with photolysis rates that are less than the frequency at which clouds form and air is processed through them ($\sim 24\,\mathrm{day}^{-1}$), the average J is the relevant quantity for chemistry modeling.

The next step would be to model at high-enough resolution so that air parcels are either cloudy or clear. This could resolve the 3-D correlation of clouds at scales of 1–4 km, which would in turn require a 3-D radiative transfer model (Norris et al., 2008; Davis and Marshak, 2010). A more interesting approach that is practical with typical global model resolution is the treatment of inhomogeneous cloud fields as being composed of independently scattering cloudlets (Petty, 2002). This cloudlet approximation could be readily integrated into the plane-parallel framework of Fast-J.

The added computational cost with G6/.33+AvQCA occurs with the additional calls to Fast-J, as the MAX-COR model and sorting of ICAs is fast. Computing photolysis rates 2.8 times per atmospheric column instead of once may add to the overall computational burden, but Fast-J is efficient and the costs should still be much less than the overall chemistry-solver and tracer-transport codes.

Code availability

The most recent version of Cloud-J and earlier versions of Fast-J can be found at ftp://128.200.14.8/public/prather/fastJX/. Cloud-J 7.3 as described here is included as a zip-file with the supplementary material of this publication. Subscribe to the maillist UCI-Fast-J@uci.edu or check the ftp site for updates on cross sections following new evaluations of photochemical data.

The Supplement related to this article is available online at doi:10.5194/gmdd-8-4051-2015-supplement.

GMDD
8, 4051–4073, 2015

Acknowledgements. Research at UCI was supported by NASA grant NNX13AL12G and DOE BER award DE-SC0012536.

References

Atkinson, R., Baulch, D. L., Cox, R. A., Crowley, J. N., Hampson, R. F., Hynes, R. G., Jenkin, M. E., Rossi, M. J., Troe, J., and Wallington, T. J.: Evaluated kinetic and photochemical data for atmospheric chemistry: Volume IV – gas phase reactions of organic halogen species, Atmos. Chem. Phys., 8, 4141–4496, doi:10.5194/acp-8-4141-2008, 2008.

Bian, H. S. and Prather, M. J.: Fast-J2: accurate simulation of stratospheric photolysis in global chemical models, J. Atmos. Chem., 41, 281–296, 2002.

Blitz, M. A., Heard, D. E., and Pilling, M. J.: Study of acetone photodissociation over the wavelength range 248–330 nm: evidence of a mechanism involving both the singlet and triplet excited states, J. Phys. Chem. A, 110, 6742–6756, doi:10.1021/Jp056276g, 2006.

Briegleb, B. P.: Delta-Eddington Approximation for solar-radiation in the NCAR Community Climate Model, J. Geophys. Res., 97, 7603–7612, 1992.

Davis, A. B. and Marshak, A.: Solar radiation transport in the cloudy atmosphere: a 3-D perspective on observations and climate impacts, Rep. Prog. Phys., 73, 026801, doi:10.1088/0034-4885/73/2/026801, 2010.

Emmons, L. K., Apel, E. C., Lamarque, J.-F., Hess, P. G., Avery, M., Blake, D., Brune, W., Campos, T., Crawford, J., DeCarlo, P. F., Hall, S., Heikes, B., Holloway, J., Jimenez, J. L., Knapp, D. J., Kok, G., Mena-Carrasco, M., Olson, J., O'Sullivan, D., Sachse, G., Walega, J., Weibring, P., Weinheimer, A., and Wiedinmyer, C.: Impact of Mexico City emissions on regional air quality from MOZART-4 simulations, Atmos. Chem. Phys., 10, 6195–6212, doi:10.5194/acp-10-6195-2010, 2010.

Feng, Y., Penner, J. E., Sillman, S., and Liu, X.: Effects of cloud overlap in photochemical models, J. Geophys. Res., 109, D04310, doi:10.1029/2003JD004040, 2004.

Fu, T. M., Jacob, D. J., Wittrock, F., Burrows, J. P., Vrekoussis, M., and Henze, D. K.: Global budgets of atmospheric glyoxal and methylglyoxal, and implications for formation of secondary organic aerosols, J. Geophys. Res., 113, D15303, doi:10.1029/2007JD009505, 2008.

GMDD

8, 4051–4073, 2015

Galloway, M. M., Loza, C. L., Chhabra, P. S., Chan, A. W. H., Yee, L. D., Seinfeld, J. H., and Keutsch, F. N.: Analysis of photochemical and dark glyoxal uptake: implications for SOA formation, Geophys. Res. Lett., 38, L17811, doi:10.1029/2011GL048514, 2011.

Horowitz, L. W., Liang, J. Y., Gardner, G. M., and Jacob, D. J.: Export of reactive nitrogen from North America during summertime: sensitivity to hydrocarbon chemistry, J. Geophys. Res., 103, 13451–13476, 1998.

Hsu, J. N. and Prather, M. J.: Is the residual vertical velocity a good proxy for stratosphere–troposphere exchange of ozone?, Geophys. Res. Lett., 41, 9024–9032, doi:10.1002/2014gl061994, 2014.

Ito, A., Sillman, S., and Penner, J. E.: Effects of additional nonmethane volatile organic compounds, organic nitrates, and direct emissions of oxygenated organic species on global tropospheric chemistry, J. Geophys. Res., 112, D06309, doi:10.1029/2005JD006556, 2007.

Ito, A., Sillman, S., and Penner, J. E.: Global chemical transport model study of ozone response to changes in chemical kinetics and biogenic volatile organic compounds emissions due to increasing temperatures: sensitivities to isoprene nitrate chemistry and grid resolution, J. Geophys. Res., 114, D09301, doi:10.1029/2008jd011254, 2009.

Jacob, D. J., Logan, J. A., Yevich, R. M., Gardner, G. M., Spivakovsky, C. M., Wofsy, S. C., Munger, J. W., Sillman, S., Prather, M. J., Rodgers, M. O., Westberg, H., and Zimmerman, P. R.: Simulation of summertime ozone over North-America, J. Geophys. Res., 98, 14797–14816, 1993.

Joseph, J. H., Wiscombe, W. J., and Weinman, J. A.: Delta-Eddington Approximation for radiative flux-transfer, J. Atmos. Sci., 33, 2452–2459, 1976.

Kato, S., Sun-Mack, S., Miller, W. F., Rose, F. G., Chen, Y., Minnis, P., and Wielicki, B. A.: Relationships among cloud occurrence frequency, overlap, and effective thickness derived from CALIPSO and CloudSat merged cloud vertical profiles, J. Geophys. Res., 115, D00H28, doi:10.1029/2009JD012277, 2010.

Naud, C. and DelGenio, A. D.: Cloud Overlap Dependence on Atmospheric Dynamics, Sixteenth ARM Science Team Meeting Proceedings, 27–31 March 2006, Albuquerque, NM, 2006.

Neu, J. L., Prather, M. J., and Penner, J. E.: Global atmospheric chemistry: integrating over fractional cloud cover, J. Geophys. Res., 112, D11306, doi:10.1029/2006JD008007, 2007.

GMDD
8, 4051–4073, 2015

Norris, P. M., Oreopoulos, L., Hou, A. Y., Taod, W.-K., and Zenga, X.: Representation of 3-D heterogeneous cloud fields using copulas: theory for water clouds, Q. J. Roy. Meteor. Soc., 134, 1843–1864, 2008.

Oreopoulos, L., Lee, D., Sud, Y. C., and Suarez, M. J.: Radiative impacts of cloud heterogeneity and overlap in an atmospheric General Circulation Model, Atmos. Chem. Phys., 12, 9097–9111, doi:10.5194/acp-12-9097-2012, 2012.

Petty, G. W.: Area-average solar radiative transfer in three-dimensionally inhomogeneous clouds: the Independently Scattering Cloudlet Model, J. Atmos. Sci., 59, 2910–2929, 2002.

Pincus, R., Hannay, C., Klein, S. A., Xu, K.-M., and Hemler, R.: Overlap assumptions for assumed probability distribution function cloud schemes in large-scale models, J. Geophys. Res., 110, D15S09, doi:10.1029/2004JD005100, 2005.

Sander, S. P., Friedl, R. R., Abbatt, J. P. D., Barker, J. R., Burkholder, J. B., Golden, D. M., Kolb, C. E., Kurylo, M. J., Moortgat, G. K., Wine, P. H., Huie, R. E., and Orkin, V. L.: Chemical Kinetics and Photochemical Data for Use in Atmospheric Studies, Evaluation No. 17, Jet Propulsion Laboratory, Pasadena, CA, 2011.

Slobodda, J., Hünerbein, A., Lindstrot, R., Preusker, R., Ebell, K., and Fischer, J.: Multichannel analysis of correlation length of SEVIRI images around ground-based cloud observatories to determine their representativeness, Atmos. Meas. Tech., 8, 567–578, doi:10.5194/amt-8-567-2015, 2015.

Søvde, O. A., Prather, M. J., Isaksen, I. S. A., Berntsen, T. K., Stordal, F., Zhu, X., Holmes, C. D., and Hsu, J.: The chemical transport model Oslo CTM3, Geosci. Model Dev., 5, 1441–1469, doi:10.5194/gmd-5-1441-2012, 2012.

Stamnes, K., Tsay, S. C., Wiscombe, W., and Jayaweera, K.: Numerically stable algorithm for discrete-ordinate-method radiative-transfer in multiple-scattering and emitting layered media, Appl. Optics, 27, 2502–2509, 1988.

Tie, X. X., Madronich, S., Walters, S., Zhang, R. Y., Rasch, P., and Collins, W.: Effect of clouds on photolysis and oxidants in the troposphere, J. Geophys. Res., 108, 4642, doi:10.1029/2003jd003659, 2003.

Wild, O., Zhu, X., and Prather, M. J.: Fast-J: accurate simulation of in- and below-cloud photolysis in tropospheric chemical models, J. Atmos. Chem., 37, 245–282, 2000.

GMDD
8, 4051–4073, 2015

Table 1. Models for cloud overlap and approximation of ICAs including errors in *J* values.

Cloud overlap models to generate ICAs		ICAs[a]	avg err 0–1 km		rms err 0–1 km		rms err 0–16 km	
			J-O^1D	J-NO_3	J-O^1D	J-NO_3	J-O^1D	J-NO_3
G0	MAX-RAN with MAX groups bounded by layers with CF = 0	19	+2 %	+2 %	21 %	17 %	6 %	11 %
G3	3 MAX-RAN groups split at 1 km and at the ice-only cloud level	21	+2 %	+2 %	15 %	15 %	5 %	7 %
G6/.00	6 MAX-COR groups, cc = 0.00	169	−1 %	−1 %	5 %	4 %	2 %	3 %
G6/.33	6 MAX-COR groups, cc = 0.33[b]	169						
G6/.99	6 MAX-COR groups, cc = 0.99	169	+2 %	+1 %	11 %	8 %	4 %	7 %
Simple cloud models		**ICAs**						
ClSky	clear sky, ignore clouds	1	+14 %	+10 %	24 %	20 %	14 %	23 %
AvCld	average fractional cloud across layer	1	−5 %	+1 %	11 %	11 %	8 %	15 %
CF3/2	increase CF to $CF^{3/2}$ and average over layer	1	+7 %	+11 %	10 %	15 %	5 %	8 %
ICA approximations		**J calls**						
AvDir	average direct beam from all ICAs	1	+5 %	+11 %	6 %	13 %	3 %	7 %
MdQCA	Quadrature Column Atmospheres uses mid-point in each QCA	2.8	+1 %	0 %	4 %	4 %	4 %	5 %
AvQCA	QCAs, uses average in each QCA	2.8	−1 %	0 %	3 %	2 %	2 %	4 %
Ran-3	Select 3 ICAs at random	3	+2 %	+1 %	12 %	12 %	9 %	12 %

[a] Average number of ICAs for a tropical atmosphere, see Fig. 2.
[b] Recommended cloud overlap model and reference model for calculation of errors.

GMDD
8, 4051–4073, 2015

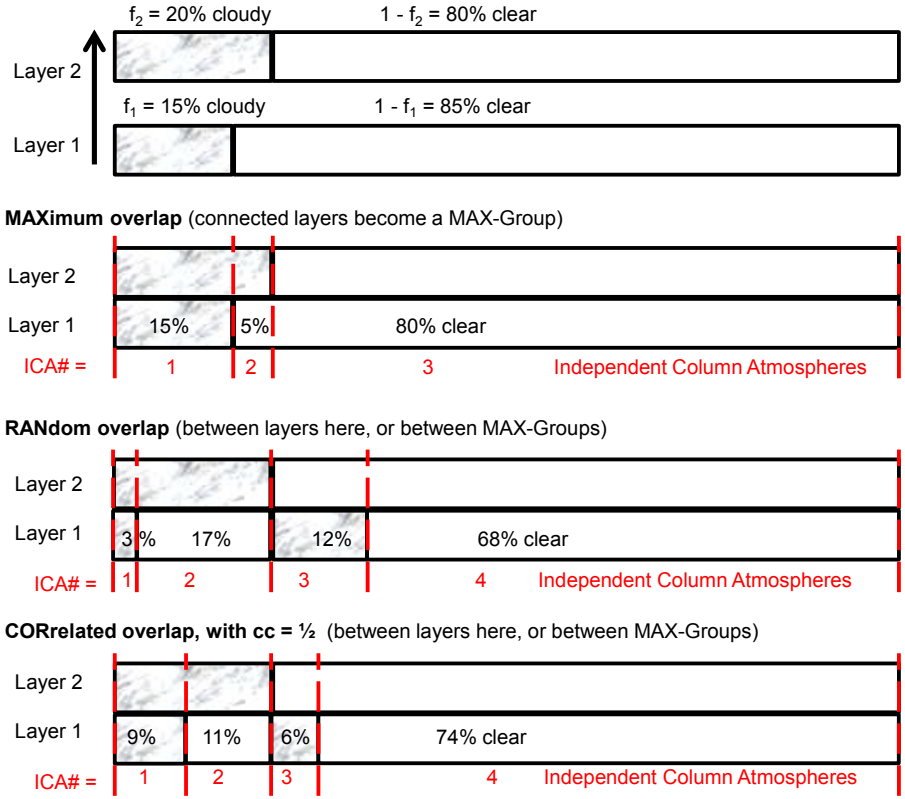

Figure 1. Schematic of overlapping fractional-cloud layers. See text.

GMDD
8, 4051–4073, 2015

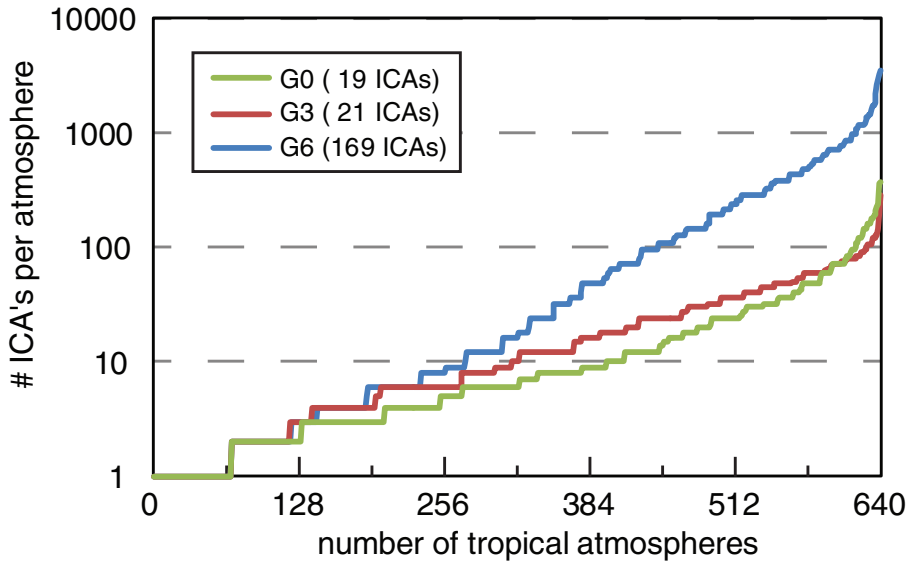

Figure 2. Number of Independent Column Atmospheres (ICAs) generated by three different cloud overlap models (G0, G3, G6) from 640 different tropical fractionally cloudy atmospheres (FCAs) and sorted in order of increasing ICA number. The different correlation coefficients used in the G6 model do not change the number of ICAs, only their weights. The average number of ICAs per FCA is given in the legend. See text for definition of models.

GMDD
8, 4051–4073, 2015

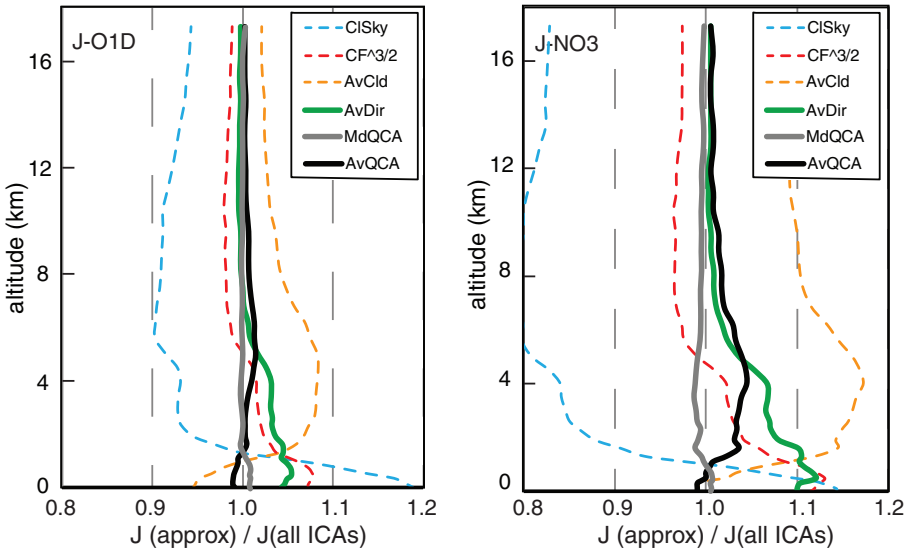

Figure 3. Profile of the average bias in J value approximations relative to the J value calculated from the weighted average of all ICAs using model G6/.33. Values here are the average of 640 FCAs (108,125 ICAs) derived from the equatorial statistics (all longitudes) of cloud fraction, liquid water content, and ice water content from a snapshot of a T319L60 meteorology from the European Centre for Medium-range Weather Forecasts. Three simple cloud methods (dashed lines) do not use any cloud-overlap model, and three approximations for the ICAs (solid lines) use the G6/.33 model described here. The MdQCA ICA approximation was developed in Neu et al. (2007); the AvQCA and AvDir approximations are developed in this paper. The J-O^1D refers to the photolysis rate of $O_3 + h\nu \Rightarrow O_2 + O(^1D)$, with average values of 4 ($z = 0$ km) to 9 ($z = 16$ km) $\times 10^{-5}$ s^{-1}; and J-NO_3, to all channels of the rate $NO_3 + h\nu \Rightarrow$, with average values of 2 to 4 $\times 10^{-1}$ s^{-1}. These two J values emphasize sunlight from 310 to 600 nm, respectively, and thus span the typical range of errors in tropospheric photolysis rates.

GMDD
8, 4051–4073, 2015

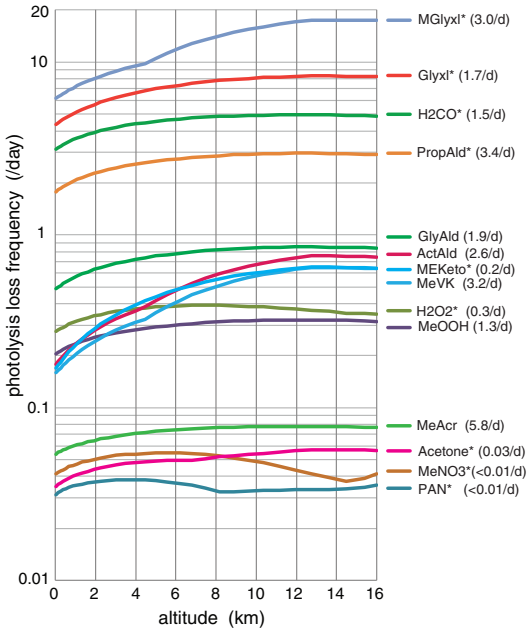

Figure 4. Volatile organic compounds (VOCs) and related species photolysis rates (day^{-1}) as a function of altitude (km). The complex structure with altitude is due to a combination of increasing UV-radiation with altitude and Sterm–Volmer pressure dependences on quantum yields. Changes in slope occur at the interpolation points, temperature or pressure, of the cross sections. We assume that the noon-time *J*'s (clear-sky, tropical atmosphere, albedo = 0.10, SZA = 15°) apply for 8 of 24 h. Equivalent rates for OH loss are shown with the species name in the legend and assume a noontime OH density of 6×10^6 cm^{-3}. Asterisks denote species for which photolysis loss is greater than or comparable to OH loss. VOC abbreviations are: MGlyxl = methyl glyoxal; Glyxl = glyoxal; PropAld = propionaldehyde; GlyAld = glycol aldehyde; ActAld = acetaldehyde; MEKeto = methylethyl ketone; MeVK = methylvinyl ketone; MeOOH = CH_3OOH; MeAcr = methacrolein; $MeNO_3$ = methyl nitrate; PAN = peroxyacetyl nitrate.

GMDD
8, 4051–4073, 2015